The impulsive tsunami source of the 2011 Off the Pacific Coast of Tohoku Earthquake estimated from seismic wave and offshore tsunami data

by

Yutaka Hayashi[1], Hiroaki Tsushima[2], Yasuhiro Yoshida[3], Takashi Yokota[4]

ABSTRACT

Offshore tsunami waveform data suggested that the maximum-amplitude tsunami at Tohoku district brought by the 2011 Off the Pacific Coast of Tohoku Earthquake was relatively short-period. By comparison of seismic and tsunami source models, we conclude that the source of tsunami with this short-period and large amplitude, namely impulsive tsunami, probably was generated in the area from the epicenter to the Japan Trench offshore.

KEYWORDS: Impulsive Tsunami Source, 2011 Off the Pacific Coast of Tohoku Earthquake, Strong Motion Waveform Inversion, Tsunami Back-propagation, Tsunami Waveform Inversion

1. INTRODUCTION

A massive *Mw*9.0 earthquake occurred at 14:46 JST (05:46 UTC) on March 11, 2011, off the Pacific coast of the northeastern part of Honshu, Japan; it is named the 2011 off the Pacific coast of Tohoku Earthquake (abbreviated as 2011 Tohoku earthquake hereinafter in this paper) by Japan Meteorological Agency (JMA) [1]. Its epicenter was southeast of Sendai City (38°06.2'N, 142°51.6'E) [2]. Seismic intensity of 7, the upper limit of JMA scale, was observed, for only the second time since JMA introduced instrument-based intensity observations in 1996 [3,4]. Intensities of 6-upper and 6-lower were widely observed at many stations in the Tohoku and Kanto districts, over an area of approximately 400km x 100km [4].

The tsunami that accompanied the earthquake detected at various offshore observation stations including coastal wave gauges [5, 6], real-time kinematic global positioning system (RTK-GPS) buoys [7] (Kato et al., 2005), cabled deep ocean-bottom pressure gauges (OBPG) (e.g. [8, 9]), and Deep-ocean Assessment and Reporting of Tsunami (DART) buoys [10]. Especially, OBPGs installed off Tohoku recorded impulsive tsunami with a short-period and large amplitude [11]. Periods of the tsunami initial waves observed at offshore stations at off Hokkaido were longer than those observed at off Iwate and Miyagi. Thus, impulsive tsunami was remarkable at west side of the tsunami source area.

In this paper, following three models are compared: the source of a seismic fault model on slip distribution estimated by strong waveform inversion [12], a tsunami source area estimated from tsunami arrival time data to offshore observatories [13], and a tsunami source area deformation field analyzed by tsunami waveform inversion [14]. Then, the source location of the impulsive tsunami is discussed.

2. STRONG MOTION WAVEFORM INVERSION

The source process of the 2011 Tohoku earthquake has been estimated from regional strong motion data. The strong motion data observed at near distance from the epicenter (< 500 km) is useful to obtain the more detailed view of the source process of large earthquake compared to the teleseismic body waves. Several studies have been performed using strong motion data [e.g. 12, 15]. In this section, we have summarized the results of source process of the 2011 Tohoku earthquake obtained from strong motion waveform inversion by Yoshida *et al.* (2011) [12].

Twenty-three strong motion seismograms from K-NET [16] and KiK-net stations [17], deployed by the National Research Institute for Earth Science and Disaster Prevention (NIED), and from the JMA, were used. Acceleration

[1] Senior Researcher, the 1st Laboratory, Seismology and Volcanology Research Division, Meteorological Research Institute, Tsukuba-shi, Ibaraki-ken 305-00526 Japan

[2] Researcher, the 1st Laboratory, ditto

[3] Senior Researcher, the 2nd Laboratory, ditto

[4] Director, ditto

seismograms were integrated to velocity, then the data were band-pass filtered between 0.01 and 0.15 Hz and decimated to 0.5 Hz. We used 250 s of data, starting from 10 s before the P wave arrivals. The strike and dip angles of the fault plane was fixed at 201°and 9°, respectively. The fault size was taken to be 475 km × 175 km, and the rupture was assumed to start at the hypocenter of the mainshock determined by JMA. We divided the fault into subfaults 25 km × 25 km in size.

The Green's function for each subfault was calculated by the discrete wavenumber method [18] using the reflection-transmission matrices [19]. The anelasticity effect was included by the use of complex velocity [20]. The moment rate function for each subfault was expressed by 20 basic triangle functions with 8 s duration over-lapping by 4 s. The maximum rupture velocity was set at 2.5 km/s to minimize variance. We used the linear multiple time window inversion method with constraints on the smoothness of the spatiotemporal slip distribution [e.g. 21, 22]. The smoothness parameters (hyperparameters) were selected to minimize Akaike's Bayesian information criterion (ABIC) [23, 24]. Wave-forms were aligned by onset time and weights on waveforms were equal for all stations.

Figure 2 shows the slip distribution obtained from the regional strong motion data analysis. The total seismic moment was 3.4×10^{22} Nm ($Mw = 9.0$). The slip area extends eastward from the hypocenter to the shallower part of the fault plane. The maximum slip amount is 38 m. The overall fit between observed and synthetic waveforms is quite good with a reduction in variance of about 91%.

The history of released seismic moment is as follows. In the first stage of the rupture (0–40 s), the rupture expands outward from the hypocenter. In the next stage (40–80 s), the rupture area extends toward the shallow part of the fault plane in both north and south directions. This stage causes large slip amounts and may be related to the generation of the large tsunami. The rupture velocity is very slow (about 1 km/s) during the first and second stages. In the third stage (after 80 s), the rupture extends southward, reaching the southern end of the fault plane at 160 s.

3. BACK-PROPAGATION OF TSUNAMI ARRIVAL TIME

In this section, we have summarized the results of tsunami source area obtained by back-propagation of tsunami arrival time by Hayashi et al. (2011) [13].

The 2011 Tohoku earthquake tsunami was detected in a time-series observation data of sea-level heights or ocean-bottom pressures. Waveform data were acquired from total of 21 stations; MLIT (each coastal wave gauge and RTK-GPS buoy), JAMSTEC (stations KPG-1 and 2), ERI at the University of Tokyo (stations TM-1 and 2), JMA (stations Boso-2 and 3), NOAA (DART 21413 and 21418), and RFERHR (DART 21401). From the filtered waveforms, tsunami arrival times of each phase are manually read.

To find the edge of the tsunami source area, Huygen's principle was applied to back-propagate the tsunami from each observation station. For these calculations we used Geoware tsunami travel-time software (TTT v. 3.0) and bathymetric data at one-minute intervals (ETOPO1 [25]). The phase velocity of tsunami propagation was assumed to be equal to the square root of gravity multiplied by bathymetry. For very large earthquakes, the difference between the time of the main shock and the generation of the tsunami is not negligible [26]. Therefore, for back-propagation using tsunami arrival times, modification values are used by 1 min corresponding to a distance of 120 km from the epicenter to the contact point of the back-propagation line and the tsunami source area (Fig. 3a). This correction is to account for typical differences between the time of the main shock and the generation of the tsunami; this is almost equivalent to assuming an averaged apparent (i.e. projected to the seafloor) fault rupture velocity of 2 km/s.

The tsunami source area of the 2011 Tohoku earthquake, determined by back-propagation of tsunami arrivals from offshore observation stations, is indicated in Fig. 3a. The tsunami source area was approximately 500-km long with a maximum width of about 200 km. The eastern edge of the tsunami source area was along the west side of the Japan Trench, and the southern one was near N36°. Meanwhile, the aftershock area [1] includes the east side of the trench and the south of N36°. Sea-level observed at TM1, TM2, GPS804, GPS802, GPS803, and GPS801 started to change almost instantly with the arrival of a seismic wave at each station. Therefore, these offshore stations were within the tsunami source area.

Back-propagation methods were also applied to the primary crests to discuss the location of major seafloor uplift in the tsunami source area. However, this was done only for the primary crests observed by OBPGs and GPS buoys, in order to limit data to near-field tsunami in deep sea, so that using data strongly affected by non-linear effects or dispersions was avoided as much as possible.

Back-propagation curves of the primary crests observed during the 2011 Tohoku earthquake tsunami are indicated in Fig. 3. All curves, except those from GPS807 and GPS806, go through the area near N38◦ E143.5◦ surrounded by the gray dotted line in Fig. 3b. The area is several tens of kilometers east away from the epicenter. If the seafloor uplift area identified was confined only within the small area through which most back-propagation curves of the primary crests go (Fig. 3b), most of the arrival-time data of the primary crests observed at GPS buoys or OBPGs can be reasonably explained.

However, this is but one of the possible solutions which can explain the timing of the primary crests, from following reasons.

One reason is, of course, that uplifted area from a great earthquake such as the 2011 Tohoku Earthquake may be excited at multiple locations (e.g. more than one seafloor uplifted area) in the source area. In this case, it may be difficult to find the location of the maximum uplift area from the back-propagation curves of the primary crests from each station.

The other reason is that the back-propagation analysis is based on the assumption that the tsunami phase-velocity is equal to the square root of gravity multiplied by bathymetry. Nonlinearity of the phase velocity results in wave crests moving faster than this assumption; on the other hand, dispersion results in crests moving slower. These effects may cause some estimation errors in the highly-uplifted area.

The latter reason might be why it is difficult to explain the back-propagation curves from GPS807 and GPS806 (Fig. 3), unless the seafloor-uplift area has some extension in the north-to-south direction, instead of assuming the only seafloor uplift exists east of the epicenter.

4. TSUNAMI WAVEFORM INVERSION

Tsunami waveform inversion is a technique to determine a tsunami source, which is a spatial distribution of earthquake fault slip or that of an initial sea-surface displacement, from observed tsunami waveforms by a least-square approach. Many studies have applied this technique to the records of the past tsunami events [27, 28, 29, 30], as well as the 2011 Tohoku earthquake [31], and found the source characteristics of those earthquakes. Furthermore, a couple of studies have proposed a tsunami forecasting algorithm based on inversion of offshore tsunami waveforms [14, 32, 33, 34]. In this section, we have summarized the results of tsunami source region of the 2011 Tohoku earthquake by tsunami waveform inversion by Tsushima et al. (2011) [14].

The huge tsunami generated by the 2011 Tohoku earthquake was recorded at several offshore tsunami stations as shown in Fig. 1. Tsunami waveforms observed at offshore provide a tsunami source signature without distortions due to complex coastal topography [35]. Taking the advantage, in our tsunami inversion we used the offshore tsunami waveform data acquired at the four ocean bottom pressure gauges (OBPGs) and five GPS buoys deployed at offshore around Japan, meaning near-field tsunami data (Figs. 4a and 4b). The impulsive tsunami was recorded at OBPG stations TM1 and TM2, and GPS buoys 802 and 804. It is noteworthy that the only parts of waveform data which had been available on real-time basis were used in our tsunami inversion.

We estimated the distribution of an initial sea-surface displacement as tsunami source model. The inversion method applied here is a part of a tsunami forecasting algorithm developed by his previous study [34]. In the inversion, two constraints are imposed to stabilize the solution of an inverse problem. One is smoothing and the other is damping constraint. The damping constraint is based on *a prori* information that an initial sea-surface displacement due to a tsunamigenic earthquake should be zero if the epicenter is far enough away. The tsunami Green's functions were computed by the finite-difference approximation of the linear long-wave equations [36].

The comparison between the observed tsunami waveforms and the calculations shows good agreement (Figs. 4a and 4b). The uplifted area estimated by the tsunami inversion is distributed circularly from the epicenter to the trench (Fig. 4c). It is difficult to determine the more accurate location and extent of the source area of the impulsive tsunami because the azimuthal coverage of the offshore stations is not sufficient [14], but the result indicates the possibility that the significantly elevated sea-surface source is located within and/or around the estimated elevation area near the trench.

5. DISCUSSION AND CONCLUSIONS

The impulsive tsunami waves are corresponding to the primary crests detected at offshore observatories located off the Pacific coast of Tohoku district (Fig. 1). Tsunami waveform inversion determined highly-uplifted area from the epicenter to the trench (Section 4 and Fig. 4c). And, as described in Section 3, if highly-uplifted area exists between epicenter and the trench (Fig. 3b), timings of the primary crests observed at most offshore stations. In addition, the area of large slip obtained from the inversion of seismic strong-motion waves [12] is almost coincident with the area marked in Fig.3b and highly-uplifted area in Fig.4b.

Therefore, we conclude that the origin of the impulsive tsunami, which brought initial high tsunami to the Pacific coast of Tohoku, probably was from the epicenter to the Japan Trench.

6. REFERENCES

[1] Hirose, F., K. Miyaoka, N. Hashimoto, T. Yamazaki, and M. Nakamura, Outline of the 2011 off the Pacific coast of Tohoku Earthquake (*Mw* 9.0)—Seismicity: foreshocks, mainshock, aftershocks, and induced activity—, *Earth Planets Space*, **63**, 2011 (in print).

[2] Japan Meteorological Agency, *Monthly Report on Earthquakes and Volcanoes in Japan March 2011*, pp.57-148, 2011 (in Japanese).

[3] Hoshiba, M., K. Ohtake, K. Iwakiri, T. Aketagawa, H. Nakamura, and S. Yamamoto, How precisely can we anticipate seismic intensities? A study of uncertainty of anticipated seismic intensities for the Earthquake Early Warning method in Japan, *Earth Planets Space*, **62**, 611-620, 2010.

[4] Hoshiba, M., K. Ohtake, K. Iwakiri, T. Aketagawa, H. Nakamura, and S. Yamamoto, Outline of the 2011 off the Pacific coast of Tohoku earthquake (Mw9.0) ‑ earthquake early warning and observed seismic intensity –, *Earth Planets Space*, 2011 (in print).

[5] Nagai, T., Development and improvement of the Japanese coastal wave observation network (NOWPHAS), *J. Jpn. Soc. Civil. Eng.*, no. 609 (VI- 41), 1–14, 1998 (in Japanese).

[6] Nagai, T., S. Satomi, Y. Terada, T. Kato, K. Nukada, and M. Kudaka, GPS buoy and 4 seabed installed wave gauge application to offshore tsunami observation, *Proceedings of the 15th International Offshore and Polar Engineering Conference*, Volume III, 292–299, 2005.

[7] Kato, T., Y. Terada, K. Ito, R. Hattori, T. Abe, T. Miyake, S. Koshimura, and T. Nagai, Tsunami due to the 2004 September 5th off the Kii Peninsula earthquake, Japan, recorded by a new GPS buoy, *Earth Planets Space*, **57**, 279–301, 2005.

[8] Fujisawa, I., S. Tateyama, and J. Fujisaki, Permanent ocean-bottom earthquake and tsunami observation system off the Boso Peninsula, *Weath. Serv. Bull.*, **53**, 127–166, 1986 (in Japanese).

[9] Hirata, K., M. Aoyagi, H. Mikada, K. Kawaguchi, Y. Kaiho, R. Iwase, S. Morita, I. Fujisawa, H. Sugioka, K. Mitsuzawa, K. Suyehiro, H. Kinoshita, and N. Fujiwara, Real-time geophysical measurements on the deep seafloor using submarine cable in the southern Kurile subduction zone, *IEEE J. Ocean Eng.*, **27**, 170–181, 2002.

[10] González, F. I., E. N. Bernard, C. Meinig, M. C. Ebel, H. O. Mofjeld, and S. Stalin, The NTHMP tsunameter network, *Nat. Hazards*, **35**, 25–39, doi:10.1007/s11069-004-2402-4,

2005.
[11] Ito, Y., T. Tsuji, Y. Osada, M. Kido, D. Inazu, Y. Hayashi, H. Tsushima, R. Hino, and H. Fujimoto, Frontal wedge deformation near the source region of the 2011 Tohoku-Oki earthquake, *Geophys. Res. Lett.*, 2011 (in print).
[12] Yoshida, Y., H. Ueno, D. Muto, and S. Aoki, Source process of the 2011 Off the Pacific Coast of Tohoku Earthquake with the combination of teleseismic and strong motion data, *Earth Planets Space*, **63**, 2011 (in print).
[13] Hayashi, Y., H. Tsushima, K. Hirata, K. Kimura, and K. Maeda, Tsunami source area of the 2011 off the Pacific Coast of Tohoku Earthquake determined from tsunami arrival times at offshore observation station, *Earth Planets Space*, **63**, 2011 (in print).
[14] Tsushima, H., K. Hirata, Y. Hayashi, Y. Tanioka, K. Kimura, S. Sakai, M. Shinohara, T. Kanazawa, R. Hino, and K. Maeda, Near-field tsunami forecasting using offshore tsunami data from the 2011 off the Pacific coast of Tohoku Earthquake, *Earth Planets Space*, **63**, 2011 (in print).
[15] Suzuki, W., S. Aoi, and H. Sekiguchi, Source inversion analysis of the 2011/3/11 Off the Pacific Coast of Tohoku Earthquake using regional strong motion data, http://www.kyoshin.bosai.go.jp/kyoshin/topics/TohokuTaiheiyo_20110311/inversion/, 2011 (in Japanese).
[16] Kinoshita, S., Kyoshin net (K-NET), *Seism. Res. Lett.*, **69**, 209-332, 1998.
[17] Aoi, S., K. Obara, S. Hori, K. Kasahara, and Y. Okada, New Strong-Motion Observation Network: Kik-net, *EOS Trans. AGU*, p. 329, 2000.
[18] Bouchon, M., A simple method to calculate Green's functions for elastic layered media, *Bull. Seism. Soc. Am.*, **71**, 959-971, 1981.
[19] Kennett, L. N. and N. J. Kerry, Seismic waves in a stratified half space, *Geophys. J. R. Astr. Soc.*, **57**, 557-583, 1979.
[20] Takeo, M., Near-field synthetic seismograms taking into account the effect of anelasticity, *Meteorol. Geophys.*, **36**, 245-257, 1985 (in Japanese).
[21] Ide, S., M. Takeo, and Y. Yoshida, Source process of the 1995 Kobe earthquake: Determination of spatio-temporal slip distribution by Bayesian modeling, *Bull. Seismol. Soc. Am.*, **86**, 547-566, 1996.
[22] Nakayama, W. and M. Takeo, Slip history of the 1994 Sanriku-haruka-oki, Japan, earthquake deduced from strong-motion data, *Bull. Seismol. Soc. Am.*, **87**, 918-931, 1997.
[23] Akaike, H., Likelihood and the Bayes procedure, in Bayesian statics, Edited by J. M. Bernardo, M. H. DeGroot, D. V. Lindley, and A. F. M. Smith, University Press, Valencia, Spain, 1980.
[24] Fukahata, Y., Y. Yagi, and M. Matsu'ura, Waveform inversion for seismic source processes using ABIC with two sorts of prior constraints: comparison between proper and improper formulations, *Geophys. Res. Lett.*, **30**(6), 1305, doi:10.1029/2002GL016293, 2003.
[25] Amante, C. and B. W. Eakins, ETOPO1 1 arc-minute global relief model: Procedures, data source and analysis, *NOAA Technical Memorandum*, NESDIS NGDC-24, 19p, 2009.
[26] Seno, T. and K. Hirata, Did the 2004 Sumatra-Andaman earthquake involve a component of tsunami earthquakes?, Bull. *Seismol. Soc. Am.*, **97**, S296–S306, 2007.
[27] Satake, K., Inversion of tsunami waveforms for the estimation of heterogeneous fault motion of large submarine earthquakes: The 1968 Tokachi-oki and 1983 Japan Sea earthquakes, *J. Geophys. Res.*, **94**, 5627-5636, doi:10.1029/JB094iB05p05627, 1989.
[28] Tanioka, Y., Yudhicara, T. Kususose, S. Kathiroll, Y. Nishimura, S. Iwasaki, and K. Satake, Rupture process of the 2004 great Sumatra-Andaman earthquake estimated from tsunami waveforms, *Earth Planets Space*, **58**, 203-209, 2006.
[29] Fujii, Y., and K. Satake, Tsunami sources of the November 2006 and January 2007 great Kuril earthquakes, *Bull. Seism. Soc. Am.,* **98**, 1559-1571, doi:10.1785/0120070221, 2008.
[30] Saito, T., K. Satake, and T. Furumura, Tsunami waveform inversion including dispersive waves: the 2004 earthquake off Kii Peninsula, Japan, *J. Geophys. Res.*, **115**, B06303, doi:10.1029/2009JB006884, 2010.
[31] Fujii, Y., K. Satake, S. Sakai, M. Shinohara, and T. Kanazawa, Tsunami source of the

2011 off the Pacific coast of Tohoku, Japan Earthquake, *Earth Planets Space*, **63**, 2011 (in press).

[32] Titov, V. V., F. I. González, E. N. Bernard, M. C. Eble, H. O. Mojfeld, J. C. Newman, and A. J. Venturato, Real-time tsunami forecasting: Challenges and solutions, *Nat. Hazards*, **35**, 35-41, doi:10.1007/s11069-004-2403-3, 2005.

[33] Wei, Y., E. N. Bernard, L. Tang, R. Weiss, V. V. Titov, C. Moore, M. Spillane, M. Hopkins, and U. Kanoglu, Real-time experimental forecast of the Peruvian tsunami of August 2007 for U.S. coastlines, *Geophys. Res. Lett.*, **35**, L04609, doi:10.1029/2007GL032250, 2008.

[34] Tsushima, H., R. Hino, H. Fujimoto, Y. Tanioka, and F. Imamura, Near-field tsunami forecasting from cabled ocean bottom pressure data, *J. Geophys. Res.*, **114**, B06309, doi:10.1029/2008JB005988, 2009.

[35] González, F. I., E. N. Bernard, C. Meinig, M. Eble, H. O. Mofjeld, and S. Stalin, The NTHMP tsunameter network, *Nat. Hazards*, **35**, 25-39, doi:10.1007/s11069-004-2402-4, 2005.

[36] Satake K., Linear and nonlinear computations of the 1992 Nicaragua earthquake tsunami, *Pure Appl. Geophys.*, **144**, 455-470, doi:10.1007/BF00874378, 1995.

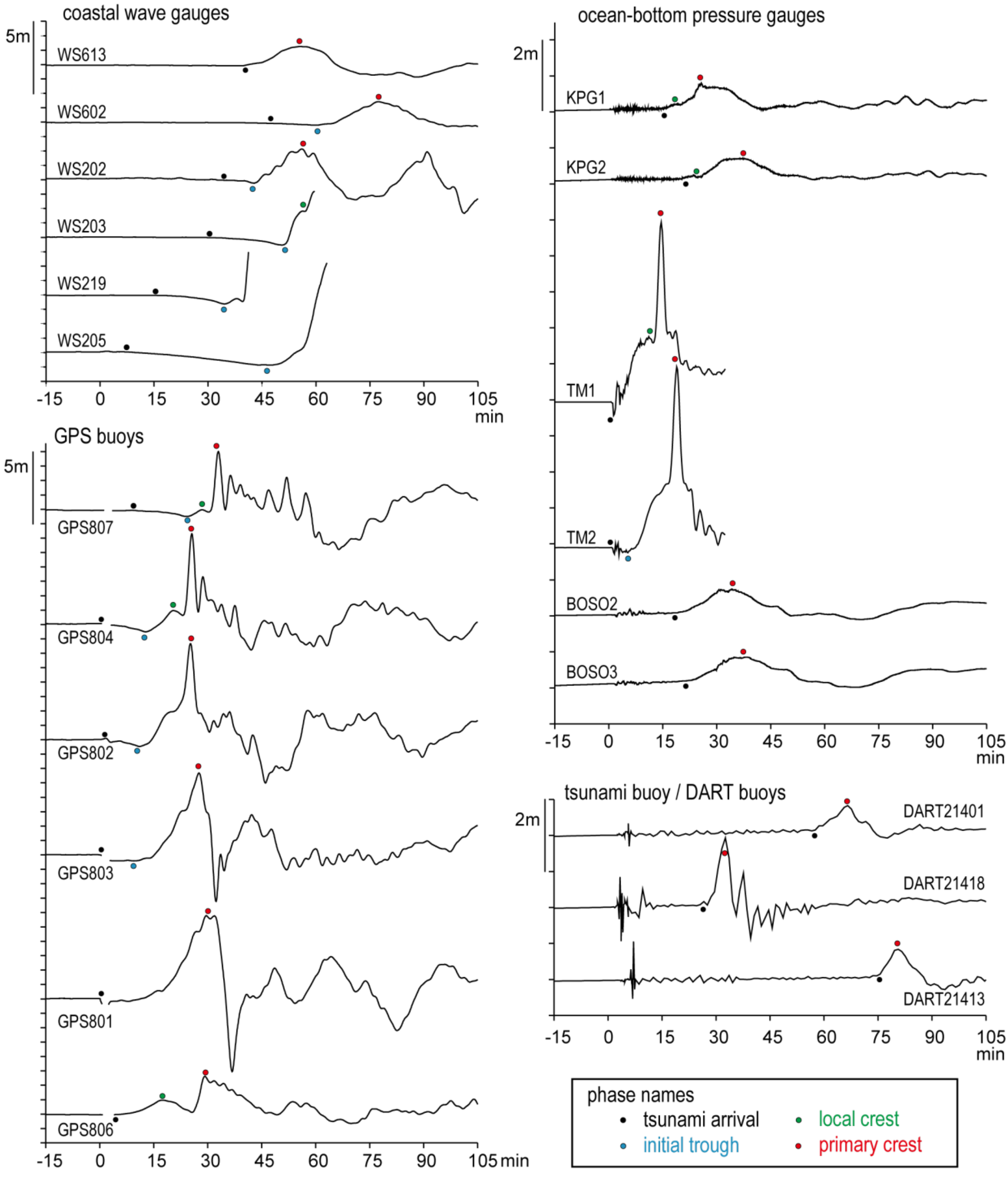

Fig. 1. Tsunami waveforms recorded offshore for the 2011 Tohoku earthquake and phase nomenclature [14]. Data are low-pass filtered. See Fig. 3 for locations of observation stations.

(a)

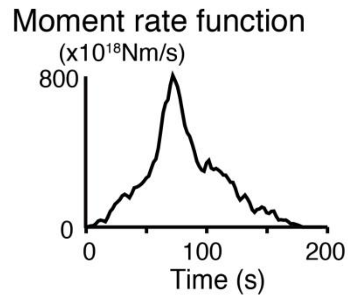

(b)

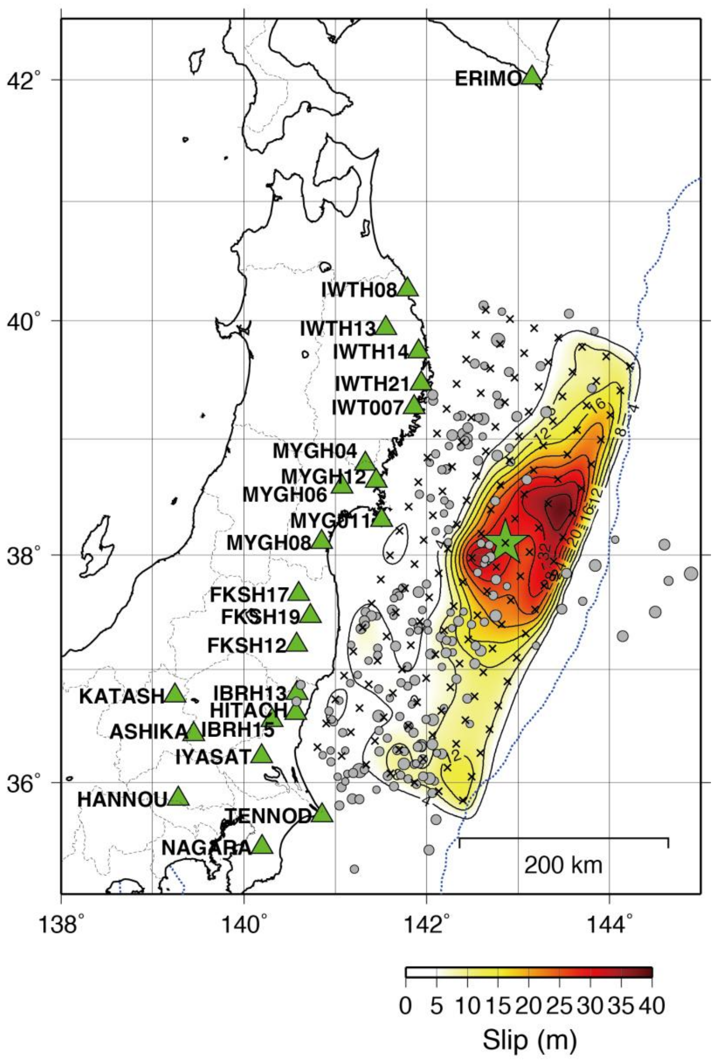

Fig. 2 Finite-source model from inversion of strong motion waves [12]. (a) Moment rate function. (b) Slip distribution on the fault. Large green star represents the epicenter of the mainshock (Mw = 9.0), and gray circles represent aftershocks (M ≥ 5.0) within 24 h of the mainshock. Crosses represent grid points on the fault plane for calculating synthetic waveforms. Triangles denote seismic stations used in this analysis. Contour interval in slip distribution is 4 m.

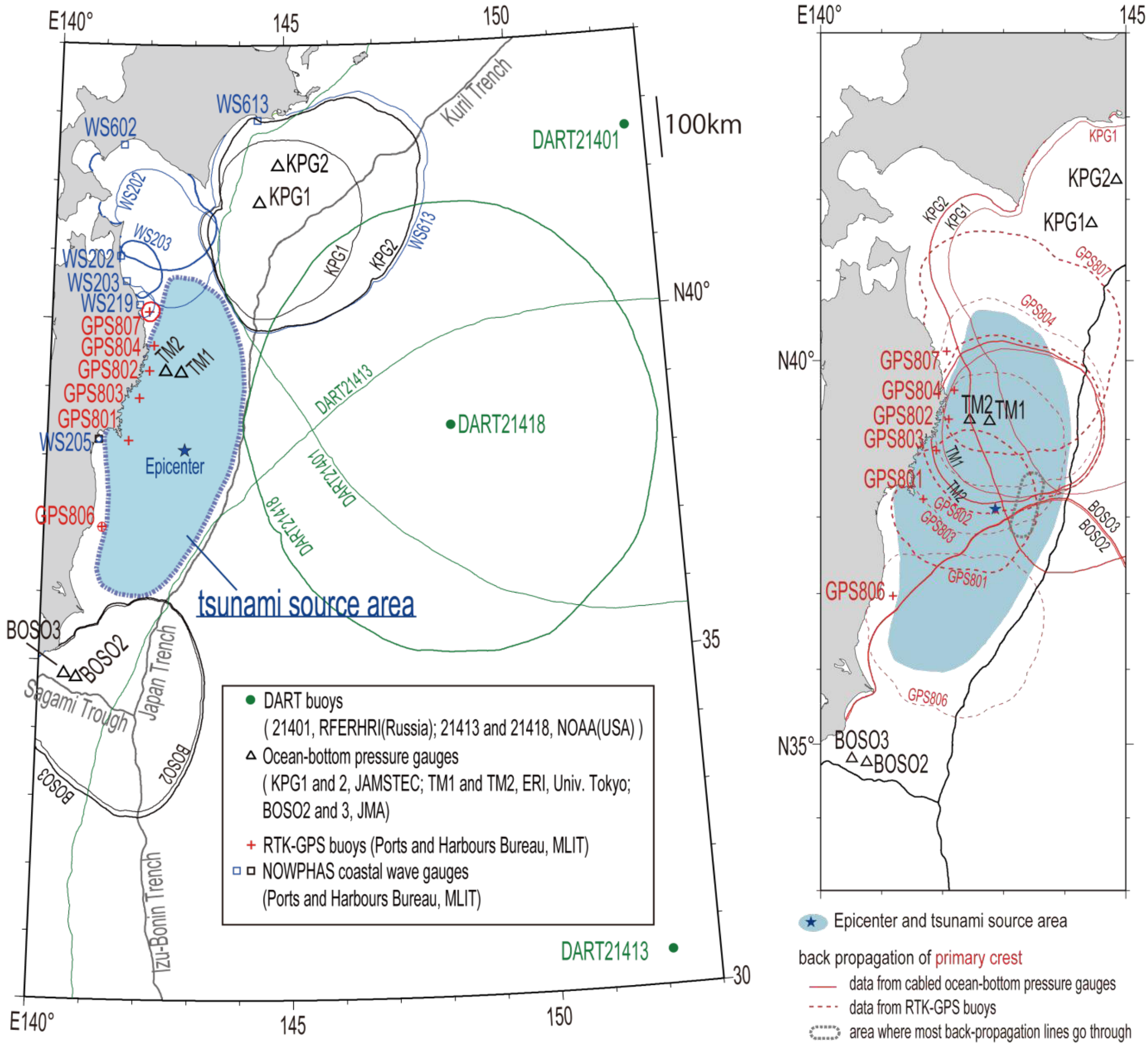

Fig. 3. Tsunami source area of the 2011 Tohoku earthquake determined by the back-propagation of tsunami arrivals (left) and occurrence times of the primary crests (right) from offshore observation stations [13].

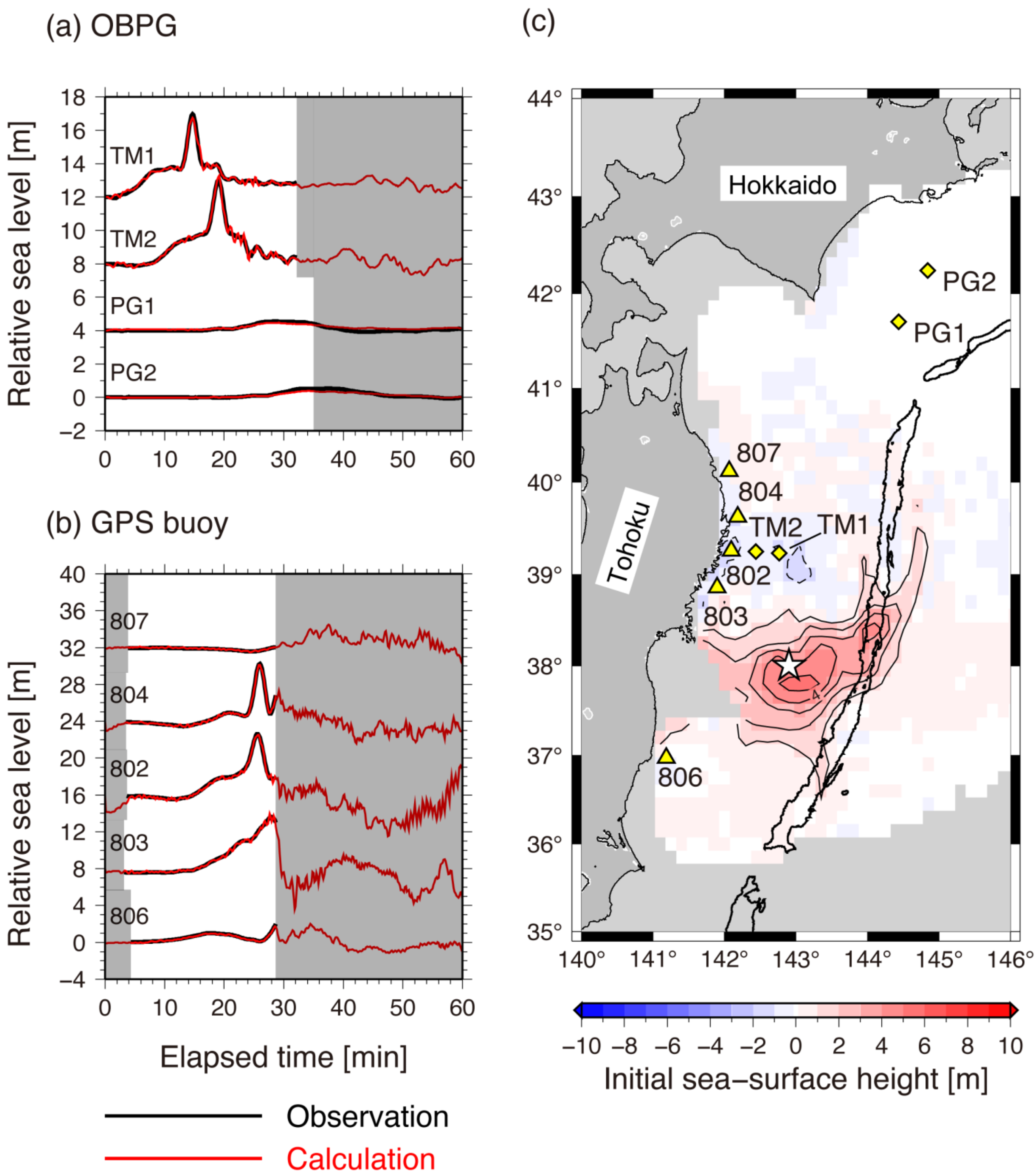

Fig. 4. Result of tsunami waveform inversion using the offshore tsunami waveforms from the 2011 Tohoku earthquake. Comparison of observed (black lines) and calculated (red lines) waveforms at (a) four OBPGs and (b) five GPS buoys. The waveforms in unshaded areas of each panel were used in the inversion. (c) Distribution of the initial sea-surface height estimated by tsunami waveform inversion. Star indicates earthquake epicenter used as the damping constraint in the inversion. Areas shaded gray are outside the influence area. Contour interval is 1 m.